ANN.BULL.RILP(1991)No.25, 221-241

A Neuro-Synaptic Model of State-Dependent EEG Wave Generation in the Subcortico-Cortical System

Kenji Itoh

Abstract

A neuro-synaptic model of the subcortico-cortical system was presented on the basis of the interaction among the infra-slow, as well as basic, rhythms of the PSPs(post-synaptic potentials) trains which emerge CSDs (current source densities) or cortical surface potentials in order to analyze the mechanism for the generation of EEG rhythms with specific state-dependent spectral patterns. The model system was simulated by two trains of positive and negative cortical surface potentials within the same period according the thalamic clock as modulated by the infra-slow rhythms of the midbrain reticular system. The simulated EEGs showed rhythmic waxing and waning sawtooth-like waves with no frequency fluctuation, but with some spectral broadband peaks at the basic repetitive frequency as well as its harmonics.

Introduction

A number of studies on brain rhythm as a candidate for the command of neural timing in human behavior have appeared since Lashley (1951) discussed "the problem of serial order in behavior incorporated in interactional as well as internal synchrony[1),2)]. The fundamental rate of such synchronous timing for performance and perceptual behavior is said to be 5 to 10Hz in normal situations, but varies in pathological conditions, e.g., it is 7Hz in stuttering, 5Hz in monotone, etc.[3),4)]

The cortical activities which generate such behavior are difficult to observe in normal human subjects, but this is possible in animals implanted with cortical electrodes. Beuyer et al. have observed cortical rhythms during attentive and quiet wakefulness in a cat which showed cortical rhythms of 35-40Hz at high vigilance, 14Hz at quiet wakefulness, and 14 - 8Hz when drowsy, but with hemispheric asymmetries in its spatio-temporal patterns[5)]. These animal cortical rhythms have been reported as having a correlation with behavioral timing[6)].

Electromagnetic signals derived from the scalp, e.g., electroencephalograms (EEGs), magnetoencephalograms (MEGs) etc., can produce some information on brain rhythms as neural timings if such signals reflect cortical activities[6)]. The EEGs/MEGs also show a rhythmic pattern, which can be divided into several frequency bands, i.e., the delta band (1-3Hz), theta band(3-7Hz), alpha band (7-14Hz) and beta band (14-28Hz). In some EEGs, several infra-slow components lower than the delta band and a fast component higher than the beta band -- i.e., the gamma band -- can be observed[7),8)].

Changes in internal and external states influence EEGs. During sleep, the delta

component is most prominent. During quiet wakefulness with eyes-closed, however, the prominent component is the alpha wave, the frequency of which correlates with brain size[9]. The prominent components are observed as local peaks with some bandwidth in the power spectrum.

Event-related changes in rhythmical EEGs during the cognitive mode have been found by Storm van Leeuven and Kamp[10]. The higher alpha components as well as the beta components increased with lower-theta enhancement, but the lower alpha and higher theta components were unchanged by presenting a number to be added in mental calculation to a number in memory.

Pfurtscheller combined data on rhythmic EEG activities and cortical functioning to investigate the correlation between human behavior and EEGs. He found that the alpha rhythm decreased about 2 sec after movement offset, and recovered about 2 sec after movement offset. Such blocking was observed also in the beta band, but with a different time course. In another study, some rhythmic component even in the alpha band were found to be movement-resistant[11].

These event-related alpha and beta blocking/enhancement studies indicate that some rhythmic components appear as solitary waves, but that others are incidental to such waves[12].

Recent applications of multielectrodes to the cortex have made it possible to obtain "micro-EEGs" which can present information on cortical activities intermediate between a single neuron firing and macro-EEGs[13]. Micro-EEGs are related to current source densities (CSDs) which are volume-ensemble activities of microscopic currents in extracellular space. CSDs are generated by the action potentials of neurons as well as by synaptic activation, but only the CSDs from excitatory synapses are observed at the cortical surface as monopolar potentials. These surface potentials may be positive or negative according to the direction and number of pairs of CSD sources and sinks.

Based on these physiological data, various models of brain rhythmicity have been proposed, such as a periodic oscillation of the local neural network in the thalamus[14] or in the cortex[15], a global standing wave in the cortex[16], a thalamic clock in the nonspecific nucleus or in the specific nucleus[17].

In the present paper, a neuro-synaptic model of the subcortico-cortical system will be presented on the basis of the interaction of positive and negative cortical surface potentials generated by CSDs originating from excitatory postsynaptic potentials (EPSPs) in order to analyze the mechanism of the formation of cortical rhythms with state-dependent spectral patterns[18].

The Model

In this model, the process of rhythmic wave formation is performed as follows.

1) The scalp EEGs are assumed to be near field surface potentials derived from CSDs analogous to the CSD drivers, i.e., EPSPs.

2) The periodic oscillation is generated in the thalamic complex, which consists of specific nuclei, including excitatory NMDA neurons, and nonspecific nuclei, including inhibitory GABAergic neurons.
3) Both nuclei, which are connected, project periodic bursts at different layers in the cortex.
4) A burst in each layer generates EPSPs with an intensity proportional to the density of the burst.
5) The CSDs from the EPSPs evoke positive or negative cortical surface potentials according to the level of the layer where the CSDs originate.
6) The thalamic process of rhythmic burst generation is modulated directly or indirectly through the nucleus basalis by infra-slow rhythms from the cholinergic midbrain reticular formation.
7) The train of isolated events which emerge from the above process form a "cortical EEG rhythm".

The EPSP can be modeled by an equivalent circuit composed of a resting membrane potential (E), resistance (1/G) and capacitance (C) as shown in Fig.1. With a conductance change in the postsynaptic membrane, the EPSP, v(t), is described by

$$dv/dt + (G + mg)v/C - mg.E/C = 0 \quad (1)$$

after conductance change ceases

$$dv/dt + G/C = 0 \quad (2)$$

where mg is a shunt conductance and G/C is the resting membrane time constant. Using an approximation of the conductance change with a composite curve of cosine and sine waves with the same frequency but with different amplitudes, the time course unit for EPSPs, V(t), is simplified as follows,

$$V(t) = \begin{cases} [1 - \cos(t/Tc)]/2 & (0 <= t < Tc) \\ \exp[- (t - Tc)/Td] & (Tc <= t) \end{cases} \quad (3)$$

where Tc is the duration of the conductance change and Td is the discharging time constant.

When the EPSP is generated repetitively, the EPSP is

$$V(t) = \begin{cases} [1 - \cos(t/Tc)]/2 & (0 <= t < Tc) \\ [\exp(- (t - Tc)/Td) - Vo]/(1 - Vo) & (Tc <= t < T) \end{cases} \quad (4)$$

$$Vo = \exp[- (T - Tc)/Td] \quad (5)$$

$$V(t + T) = V(t) \quad (6)$$

where T is the period of the repetitive stimuli[19].

The cortical surface potentials are specified by the layer of the generated EPSPs as in Fig.2. If the surface potential, Vi(t), is generated by the EPSPs in the i-th cortical layer, the summated surface potential, S(t), is

$$S(t) = \sum_{i=1}^{n} ai.Vi(t - di) \tag{7}$$

where ai and di are the amplitude and delay of Vi, respectively, and n is the number of cortical layers.

In the case where the amplitude of Vi(t) is modulated by the wave function Mi(t), the summated surface potential, S(t), is

$$S(t) = \sum_{i=1}^{n} ai.B(1 + mi.Mi(t)).Vi(t - di) \tag{8}$$

$$B(x) = \begin{cases} B(x) & (B(x) >= 0) \\ 0 & (B(x) < 0) \end{cases} \tag{9}$$

where mi is modulation depth.

The generator of the neural clock, i.e., the bursts in excitable cells, can be simplified by a relaxation oscillator[20]. One burst cycle is composed of a burst of spikes and a silent period in which an inactivation upon depolarization occurs due to the transmembrane flux of calcium through a voltage-dependent channel activated by the neuronal membrane depolarizartion. If the burst interval is T, the burst and silent periods are Tb and Ts,

$$T = Tb + Ts \tag{10}$$

When the time scale of the respective periods of bursts and silence are more than hundreds of milliseconds and tens of milliseconds, the burst cycle is nearly determined by the silent period, i.e, the time course of the calcium influx. Since the process can also be modeled by an equivalent circuit of PSP as in Fig.1, the calcium influx produces a negative or inhibitory PSP, i.e., an IPSP with the same function as explained above.

The model system, as given in Fig.3, consists of a set of five neuronal assemblies layered in the subcortico-cortical system, i.e., a cortex with several layers (CX), a specific relay nucleus (ST) with NMDA neurons, a GABAergic nonspecific nuclear system (NT), including the nucleus reticularis thalami and central thalamic complex, the cholinergic nucleus basalis (NB) and midbrain reticular formation (RF).

A train of periodic bursts is generated in the reciprocal connection system of the ST, and the ST acts as a relaxation oscillator. The NT is only a trigger of the oscillator which acts by controlling the inhibitory GABAergic output on the voltage-dependent Ca2+ channel in the ST[21]. Both the outputs of ST and NT are projected to the fourth and first layers in the cortex, respectively. The activities of ST and NT are modulated by the slow cholinergic RF directly or indirectly through NB which also projects its output to the CX.

Simulation and Results

Figure 4 shows the simulated rhythmic waves obtained with only two surface potentials from layers IV and I at various relative amplitudes (a4/a1 = 0 to 2 in (7)) but with no amplitude modulation by the RT. Two components in the repetitively summated surface potentials, i.e., a DC level and a sinusoidal wave of fundamental frequency (f_0), were extracted by spectral analysis. The model could simulate the phase shift of a rhythmic wave by controlling the V4 amplitude, but shows a reversed-direction phase shift for a long delayed V1 potential in Fig.4c compared to the short one in Fig.4a.

Figure 5 shows a result of the superimposed surface potentials of two summated surface potentials, as does Fig.4, but with various delays between the first and second summated surface potentials (0 to 360). The model system could simulate a near-sinusoid wave with a second harmonic frequency of 180 as well as the fundamental frequencies of 90 and 270.

Figure 6 shows the set of waveforms and power spectra of the summated surface potentials from the two layers shown in Fig.4, as well as a sine wave. Only in the case of positive surface potential, some line spectra at the harmonics were observed in addition to the line spectrum at the fundamental frequency of repetition, as in the case of the sine wave. When negative surface potentials were added, the higher harmonics decreased slightly.

Figure 7 shows the set of waveforms and power spectra of the summated surface potentials shown in Fig.6, but modulated by the PSP wave of an infra-slow rhythm with different Tc values in the case of various modulation depths from 0 to 200% but having the same surface potentials. The modulation in the sine wave by the infra-slow rhythm broadens the bandwidth of the peak component. The modulated surface potentials of one positive component showed such broadening at each peak component, but added a low frequency component at the modulator repetitive frequency. In the case of biphasic summated surface potentials, this low frequency component ceased. The variation in Tc values had almost no effect on the spectral characteristics.

Figure 8 shows the set of waveforms and power spectra of the summated surface potentials with a slow rhythm close to the modulator repetitive frequency. The modulation had a prominent effect on the broadening of the local spectral peaks to the extent that a series of local peaks became an almost continuous spectrum.

Discussion

A neuro-synaptic model of EEG generation was presented without using sinusoidal waves, but instead using the distorted saw-tooth-like waves with harmonics analogous to postsynaptic potentials as basic units for rhythmic EEGs, which could be simulated based on two simple interactions among a restricted number of such basic units, i.e, linear summation and amplitude modulation.

In the neuro-synaptic model of the cortico-subcortical system, a simple summated potential of only two surface potentials with the same charging duration, as well as a simple superimposed potential of two summated potentials with the same component with and without amplitude modulation by infra-slow rhythms, were adopted to explain the amplitude and phase shifts in rhythmic scalp EEG waves in the time domain as well as the state-dependent spectral change. In the case of only one summated potential, the increase in the relative amplitude of the fourth surface potential also caused a shift in the DC level, as well as in the amplitude of the fundamental wave. Thus, the model system in this case could not determine the phase and amplitude of the wave independently.

The model system with two summated surface potentials linearly superimposed could simulate the generation of a sinusoid- like wave at the second harmonic frequency with no use of a nonlinear function, as shown in Fig.5. The wave corresponds to a beta wave when the repetitive frequency of the thalamic bursts is in the alpha band, and to an alpha wave when the frequency is in the theta band. The system could, with only one summated potential in certain proper conditions, also generate a near-sinusoidal wave, but with a bit more distortion than that generated from two summated potentials.

Steriade and Llinas have investigated the electrophysiological properties of guinea-pig thalamic neurons to observe their firing patterns in two frequencies, 6 and 10 Hz[22]. Also, there exist two or more components in the alpha band[23]. Such rhythmic waves with multiple components in the alpha band can be obtained, as well as slow respiratory waves and readiness potentials, during the preparatory period for movements, e.g., utterances. Schoppernhorst et al. found two components with different coherences in promotion alpha waves with frequencies of 9 and 11 Hz[24]. However, alpha, as well as beta, waves have different spatio-temporal patterns on the scalp[25], as described in our introduction. It is now difficult to determine the respective mode for the generation of such rhythmic waves in alpha band as well as beta band.

The findings by Steriade et al., however, are restricted to the thalamic and cortical rhythm at around 10Hz for sleep spindle waves, which is hypothesized to be paced by even the nonspecific nucleus reticularis thalami[26]. Recent discoveries from awake cats by Buszaki have presented another understanding of the thalamic clock[27]. He concludes that the clock is not due to the pacemaker properties of thalamic cells, but to the an emergent network properties of the specific relay nucleus-nucleus reticularis. The clock frequency is regulated by the interplay between the NMDA channel and the calcium channel, which is the same process as in the Steriade model, but rather in the specific relay nucleus.

Hobson has proposed a reciprocal interaction model of sleep-cycle control using mutually connected units with respectively positive and negative self-feedbacks[28]. The model can generate the "Lofka-Volterra" oscillation. The frequency of the oscillation is known to be determined by long-lasting hyperpolarization after burst firing. In our present model based on the findings of Buzsaki, the thalamic networks have similar connections, which may also generate the Lofka-Volterra oscillation, but with a long-lasting hyperpolarization which is not produced by the inhibitory synaptic inputs but by an intrinsic increase in membrane permeability from the voltage-dependent calcium influx caused by the GABAergic neurotransmitters[29].

The global standing theory of Nunetz assumes that physical brain size is the determinant of the alpha frequency on the basis of physiological correlation data between the two parameters[30]. Further data analyses have indicated that the alpha frequency is determined by the brain metabolism, which also show a correlation to brain size[31]. The process of calcium ions passing through voltage-dependent channels has been found to be involved in the cellular metabolic cycle[32]. The rhythmic frequency, therefore, is dependent on the metabolic rate in the present model using the interplay of the NMDA and calcium channels[33]. If the metabolic rate is the determinant of the alpha frequency, the frequency fluctuates rather slightly during the steady-state condition in individuals, and the frequency shifts in a wide range according to the development from infant to adult[34].

The infra-slow rhythms from the mid-brain reticular system were used in this paper as modulators of the basic rhythms. Such infra-slow rhythms are found at several frequency bands, including around 1Hz[35], the respiratory frequency[36], and around 0.1Hz[37]. Some of these rhythms are generated in the local circuits of the midbrain as well as of the basal ganglia. Galcia-Rill and Skinner have found cyclic activities synchronous to locomotion rhythms at about 1Hz in the cholinergic posterior midbrain which connects to the aminergic locus coeruleus [38]. These cholinergic systems with other neurotransmitters are said to control function-related frequencies, as well as function-related states in motor activities, e.g., mastication, eye-movements, etc.[39]. The thalamic clock in our model is governed by the cholinergic system including the ventral basalis. Even in the case of quiet immobile condition, if the eyes open, commands for eye movements are sent to the cholinergic system, which inhibits the thalamic clock and alpha blocking results.

There are other neuro-synaptic circuits showing temporal rhythmic activities within the brain, e.g., the septo-hippocampal system[40] and the striato-motor system[41]. For the further analysis of the rhythmic waves relating to the human behavior[42], the interaction among these multiple generators with different rhythmic patterns[43] must be incorporated into the model[44].

Acknowledgement

The valuable suggestions of S. Niwa, K. Hiramatsu, M. Fukuda, O. Saitoh, K. Nakagome, A. Iwanami, T. Sasaki and S. Hayashida are greatfully appreciated by the author.

References

1) Lashley, K.S. (1951) The problem of serial order in behavior. In L.P. Jeffress (ed.) Cerebral mechanisms of behavior: The Hixon Symposium, Wiley: New York.
2) Byers, P. (1979) Biological rhythms as information channels in interpersonal communication behavior. In S. Weitz (ed.) Nonverbal communication (second ed.). Oxford Univ. Press: New York.
3) Shaffer, L.H. (1982) Rhythm and timing in skill. Psychol. Rev. 89, 109-122.
4) Obeso, J.A., M.R. Luquin and J. Artieda (1987) Motor manifestations of basal ganglia diseases: Pharmacological studies in humans. In M. Sandler, C. Feuerstein and B. Scatton (ed.) Neurotransmitter interactions in the basal ganglia. Raven Press: New York.
5) Bouyer, J.J., M.F. Montaron, J.M. Vahnee, M.P. Albert and A. Rougeul (1987) Anatomical localization of cortical beta rhythms in cat. Neurosci. 22, 863-869.
6) Semba, K. and B.R. Komisaruk (1984) Neural substrates of two different rhythmical vibrissal movements in the rat. Neuroscience 12, 761-774.
7) Birbaumer, N., T. Elbert, A.G.M. Canavan and B. Rockstroh (1990) Slow potentials of the cerebral cortex and behavior. Physiol. Rev. 70, 1-4.
8) Bressler, S.L. (1990) The gamma wave: A cortical information carrier ?. Trend. Neurosci. 14, 161-162.
9) Blumberg, M.S. (1989) An allometric analysis of the frequency of hippocampal theta: the significance of brain metabolic rate. Brain Behav. Evol. 34, 351-356.
10) Storm van Leeuwen, W. and A. Kamp (1973) Occurrence of beta bursts in frontal cortex during CNV paradigm. Electroenceph. Clin. Neurophysiol. S3, 95-97.
11) Pfurtscheller G. (1981) Central beta rhythm during sensorimotor activities in man. Electroenceph. Clin. Neurophysiol. 51, 253-264.
12) Boejinga P.H. and Lopes da Silva (1989) Modulation of EEG activity in the entorhinal cortex and forebrain olfactory areas during odour sampling. Brain Res. 478, 257-268.
13) Mitzdorf, U. (1985) Current source density method and application in cat cerebral cortex: investigation of evoked potentials and EEG phenomena. Physiol. Rev. 65, 37-100.
14) Van Rotterdam, A. and F.H. Lopes da Silva (1982) A model of the spatio-temporal characteristics of the alpha rhythm. Bull. Math Biol. 44, 283-305.
15) Lagerlund, T.D. and F.W. Sharbrough (1988) Computer simulation of the generation of the electroencephalogram. Electoenceph. Clin. Neurophysiol. 72, 31-40.
16) Nunetz, P.L. (1990) Localization of brain activity with electroencephalography. In S. Sato (ed.) Advances in neurology. 54: Magnetoencephalography. Raven Press: New York.
17) Steriade, M. and M. Deschenes (1984) The thalamus as a neuronal oscillator. Brain res. Rev. 8, 1-63.
18) Ehlers, C.L., T.L. Wall and M.A. Schuckit (1989) EEG spectral characteristics

following ethanol administration in young men. Electroenceph. Clin. Neurophysiol. 73, 179-187.
19) Itoh, K. (1985) A neuro-synaptic model of the auditory masking and unmasking process. Bilo. Cybern. 52, 229-235.
20) Chay, T.R. (1990) Bursting excitable cell models by a slow Ca2+ current. J. Theor. Biol. 142, 305-315.
21) Crunelli, V. and N. Leresche (1991) A role of GABAb receptors in excitation and inhibition of thalamocortical system. Trend. Neurosci.14. 16-21.
22) Steriade M. and R.R. Llinas (1988) The functional states of the thalamus and the associated neuronal interplay. Physiol. Rev. 68, 649-742.
23) Itoh, K. (1982) Analysis of speech related rhythmic EEG activities in normal verbal behavior. Proc. World Cong. Med. Physics and Biomed. Eng. 18, 13.
24) Schoppenhorst, M., F. Brauer, G. Freund, and S.T. Kubicki (1980) Coherence estimates in determining central alpha and mu activities. In G. Pfurtscheller, P. Buser, and F.H. Lopes da Silva (ed.) Rhythmic EEG activities and cortical functioning. Elsevier: Amsterdam.
25) De Toffol, B., A. Autret, S. Markabi and S. Roux (1990) Influence of lateralized sensorimotor and neuropsychological activities on electroencephalographic spectral power. Electroenceph. Clin. Neurophysiol. 75, 200-206.
26) Steriade, M., L. Domich, G. Oakson and M. Deschenes (1987) The deafferented reticular thalamic nucleus generators. J. Neurophysiol. 57, 260-273.
27) Buzsaki, G. (1991) The thalamic clock: emergent network properties. Neuroscience 41, 351-364.
28) Hobson, J.A. (1981) The reciprocal interaction model of sleep cycle control: a discussion in the light of Giuseppe Moruzzi's concepts. In O. Ponpeiano and C.A. Marsan (ed.) Brain Mechanisms and perceptual awareness, Raven Press: New York.
29) Meyer, F.B. (1989) Calcium, neuronal hyperexcitability and ischemic injury. Brain Res. Rev. 14, 227-243.
30) Nunetz, P.L. (1981) A study of origins of the time dependencies of scalp EEG: I - theoretical basis. IEEE Trans. BME-28, 271-280.
31) Kraaier, V., A.C. Van Huffel and C. Wieneke (1988) Changes in quantitative EEG and blood flow velocity due to standardized hyperventilation: a model of transient ischaemia in young human subjects. Electroenceph. Clin. Neurophysiol. 70, 377-387.
32) Singer, W. (1990) Ontogenetic self-organization and learning. In J.L. McGaugh, N.M. Weinberger and G. Lynch (ed.) Brain organization and memory: Cells, systems and circuits. Oxford University Press: New York.
33) Bekkers, J.M. and C.F. Stevens (1989) NMDA and non-NMDA receptors are co-localized at individual excitatory synapses in cultured rat hippocampus. Nature 341, 230-233.
34) Alvarez, A., P.A. Valdes, R.D. Pascual, L. Galan and R. Biscay (1989) On the structure of EEG development. Electroenceph. Clin. Neurophysiol. 73, 10-19.

35) Riekkinen, P., G. Buzsaki, P. Riekkinen Jr, H. Soininen, J. Partanen (1991) The cholinergic system and EEG slow waves. Electroenceph. Clin. Neurophysiol. 78, 89-96.
36) Grozinger, B., H.H. Kornhuber, J. Kriedel (1977) Human cerebral potentials preceding speech production, phonation, and movements of the mouth and tongue, with reference to respiratory and extracerebral potentials. Prog. Clin. Neurophysiol. 3, 87-103.
37) Roy, J.P., M. Clercg, M. Steriade, and M. Deschenes (1984) Electrophysiology of neurons of lateral thalamic nuclei in cat: mechanisms of long-lasting hyperpolarizations. J. Neurophysiol. 51, 1220-1225.
38) Galcia-Rill, E. and R.D. Skinner (1988) Modulation of rhythmic function in the posterior midbrain. Neurosci. 27, 639-654.
39) Birbaumer, V., T. Elbert, A.G.M. Canavan and B. Rockstroh (1990) Slow potentials of the cerebral cortex and behavior. Physiol. Rev. 70, 1-41.
40) Turner, D.A. (1990) Feed-forward inhibitory potentials and excitatory interactions in guinea-pig hippocampal pyramidal cells. J. Physiol. 422, 333-350
41) Rolls., E.T., S.J. Thorpe, M. Boytim, I. Szabo, and D.I. Perrett (1984) responses of striatal neurons in the behaving monkey. 3. Effects of iontophoretically applied dopamine on normal responsiveness. Neuroscience 12, 1201-1212.
42) Itoh, K. (1985) Simulated rhythmic EEG activities in a neurosynaptic model of thalamo-cortical system. Proc. XII ICMBE/V ICMP.
43) Crick, F. and C. Koch (1990) Some reflections on visual awareness. In Cold Spring Harbor Symposia on Quantitative Biology. LV: The Brain. Cold Spring Harbor Laboratory Press: New York.
44) Itoh K. (1991) A neuro-synaptic model of state-dependent EEG wave generation in subcortico-cortical system. Proc XII ICMBE/V ICMP.

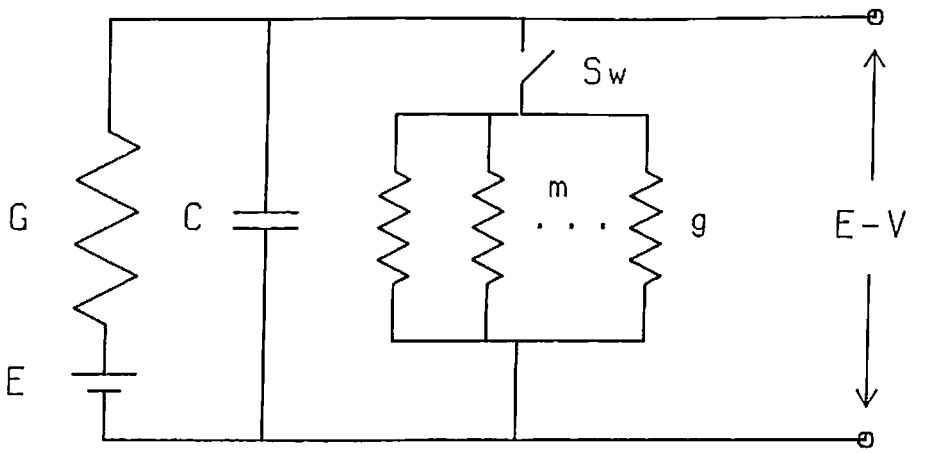

Fig.1. Electrical circuit model of the postsynaptic membrane . C: membrane capacitance; E: resting membrane conductance ; m: number of quanta transmitted by one pulse; Sw: switch of ion channel; V: postsynaptic potential[16].

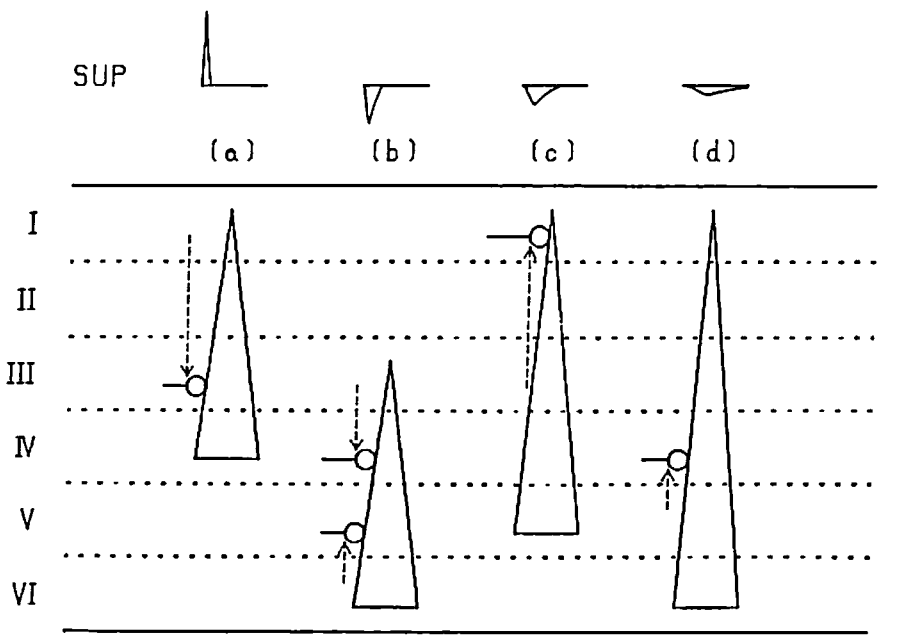

Fig.2. Current source densities (CSDs) and surface potentials evoked by EPSPs in cortical layers. SUP: surface potential; /-: cortical layers; Triangles: neurons; Circles: excitatory synapses; Arrows: CSDs (modified from[15]).

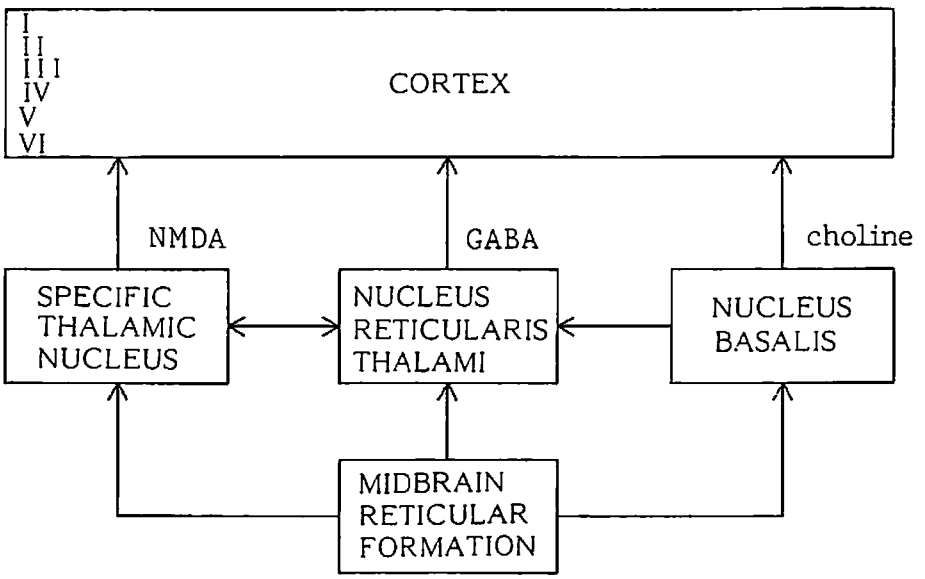

Fig.3. Block diagram of the subcortico-cortical system.

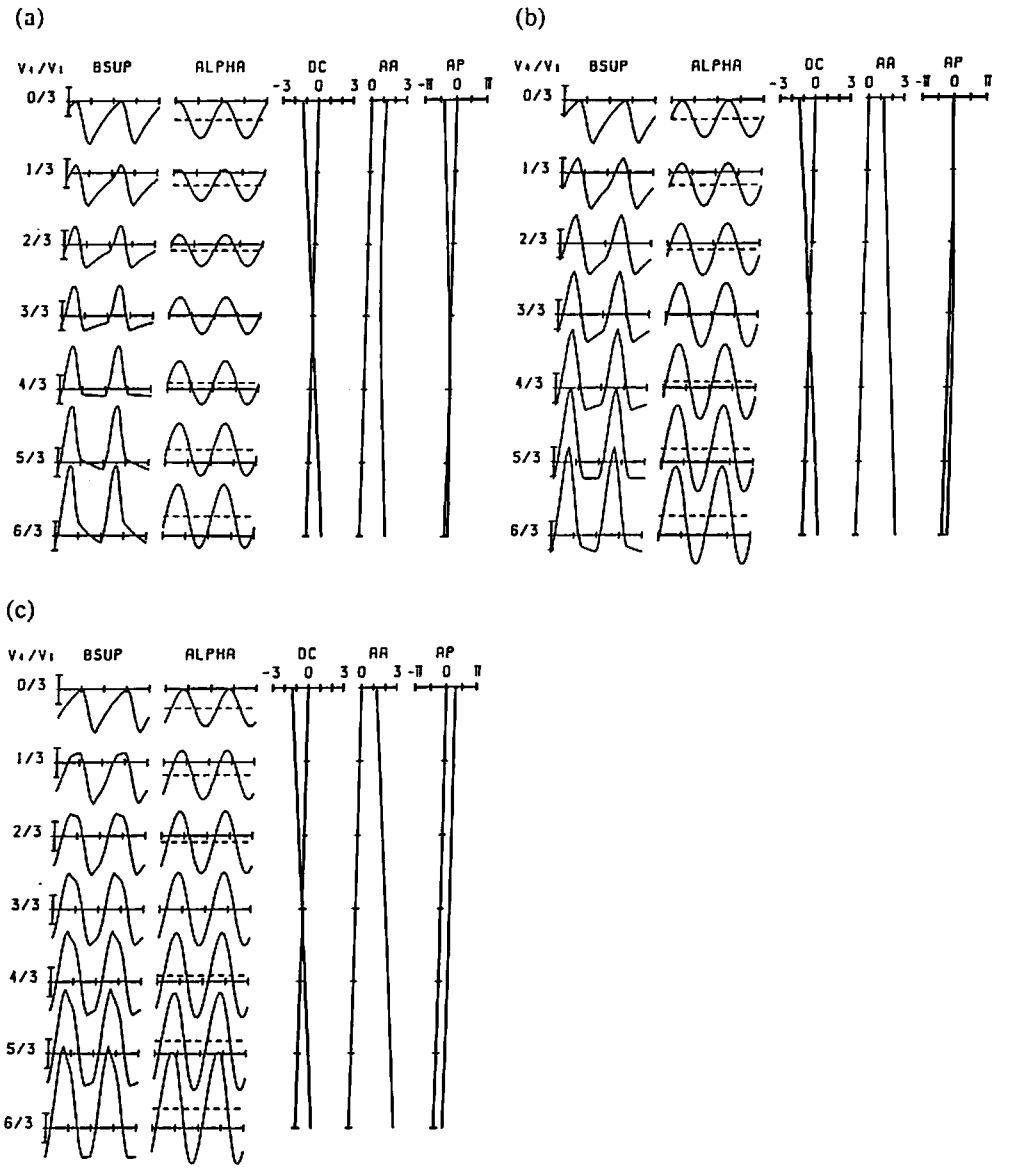

Fig.4. Rhythmic response of the system with the PSP charging duration Tc = T/3 (T: period of thalamic burst train) and discharging time constant Td = 2Tc. V4/V1: ratio of positive surface potentials (by layer I) and negative surface potential (by layer IV) amplitudes; ALPHA:DC level (broken line) and rhythmic fundamental wave (solid line) extracted from the summated surface potentials (data for two periods); DC: DC component in summated surface potentials; AA: Amplitude of fundamental rhythmic wave; AP: phase of the wave ((a):d4-d1 = T/6; (b):d4 - d1 = T/3; (c): d4 - d1 = T/2).

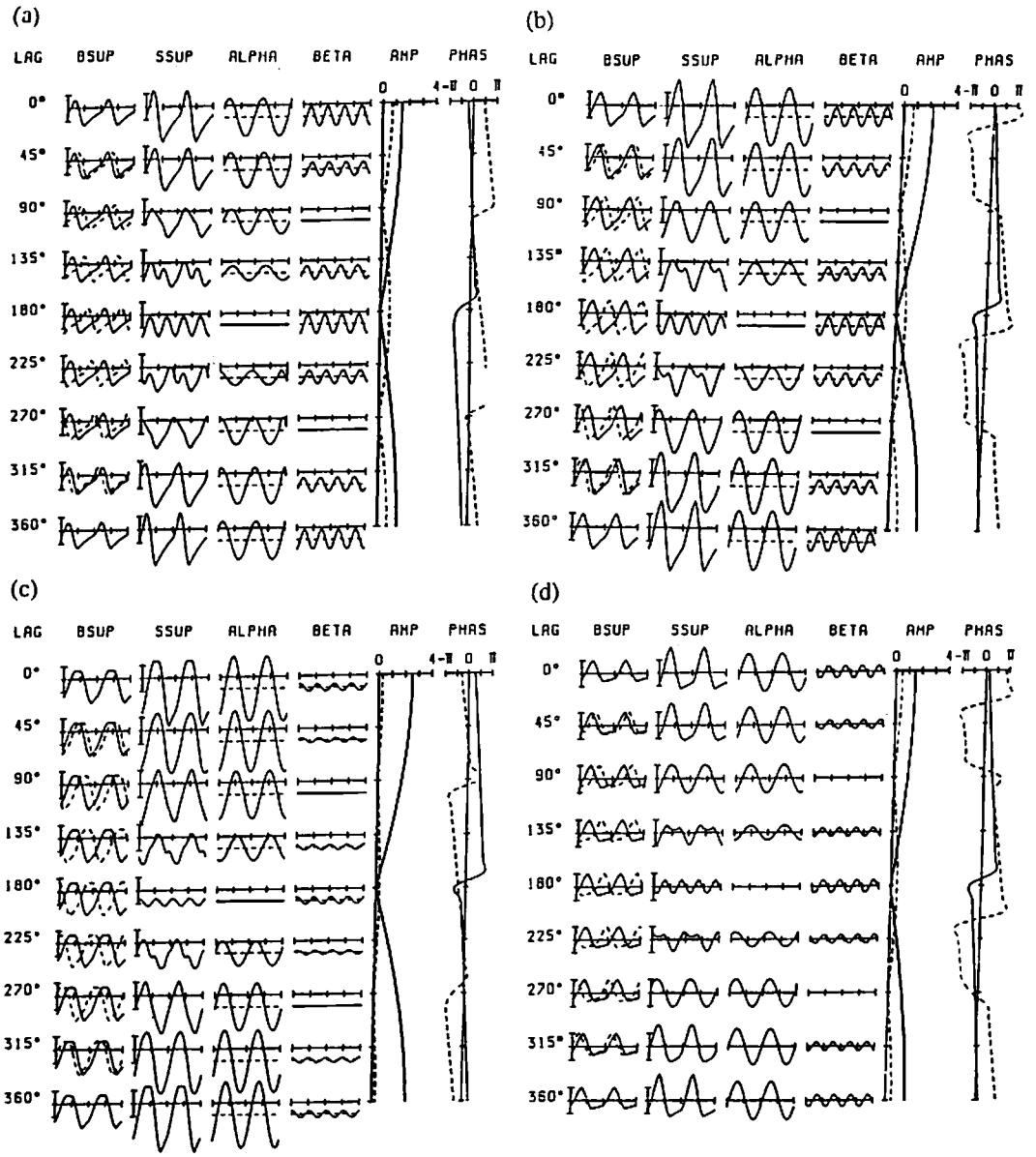

Fig.5. Rhythmic response of the system with two summated surface potentials as in Fig.4. BSUP: biphasic summated surface potential; SSUP: superimposed potential of two BSUPs with event delay (LAG) of 0 to 360_; ALPHA: DC level of (broken line) and rhythmic fundamental wave (solid line) extracted from SSUP; BETA: DC level (broken line) and rhythmic second harmonic wave (solid line) extracted from SSUP; AMP: amplitudes of fundamental wave (solid line) and second harmonic wave (broken line); PHAS: phases of fundamental wave(solid line) and second harmonic wave (broken line) ((a): a4/a1 = 1/2 and d4 - d1 = T/6 ; (b): a4/a1 = 1/2 and d4 - d1 = T/3; (c): a4/a1 = 1/2 and d4 - d1 = T/2; (d): a4/a1 = 1/1 and d4 - d1 = T/3.

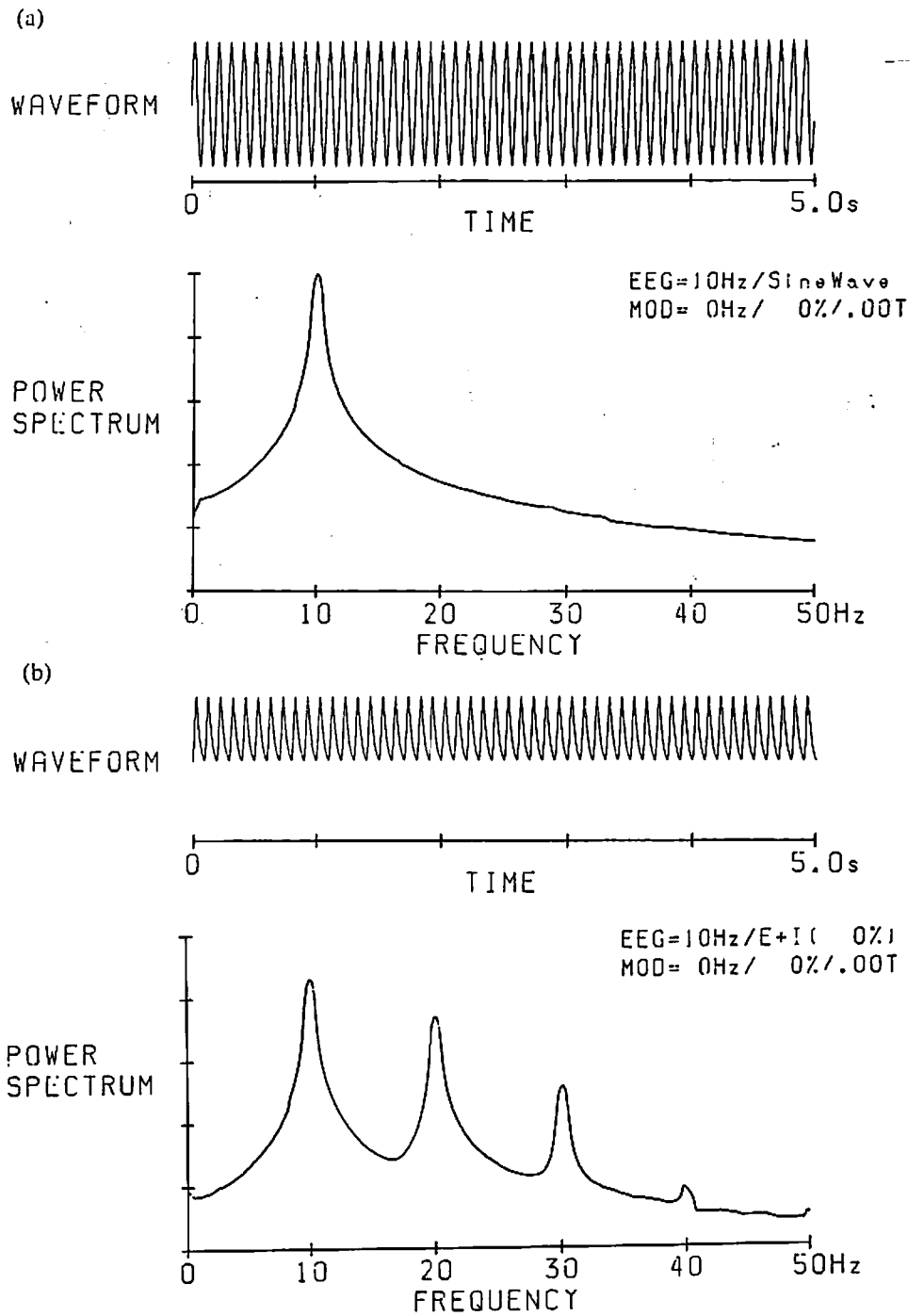

Fig.6. A set of waveforms and power spectra of the summated surface potentials of two layers as shown in Fig.4 as well as a sine wave. (a): a sinwave (0% modulation); (b): a positive surface potential (0%); (c): a biphasic surface potential (0%).

(c)

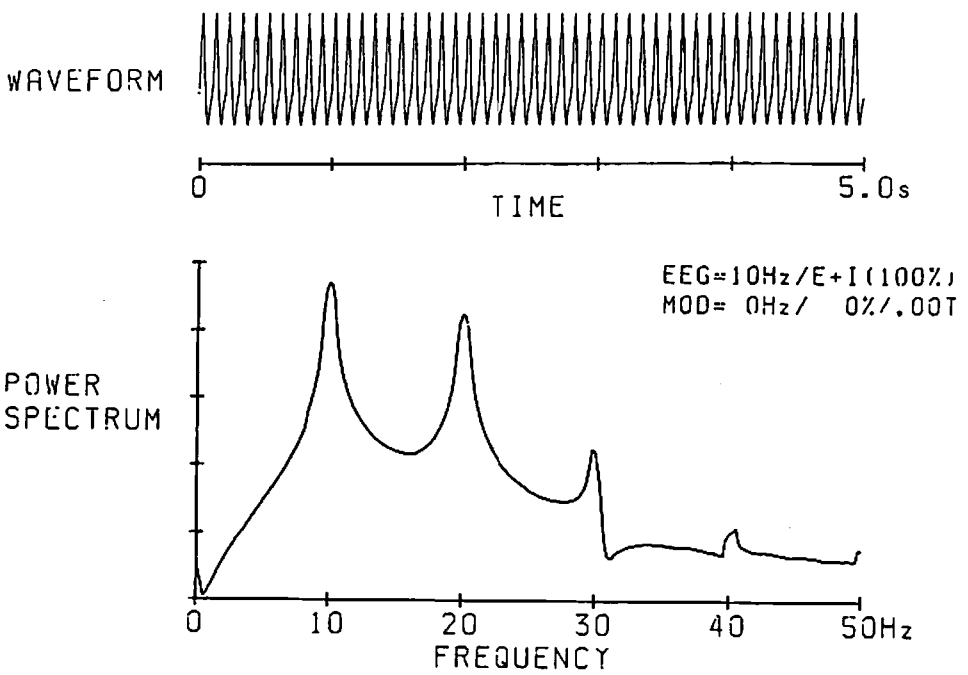
WAVEFORM
0
TIME
5.0s
EEG=10Hz/E+I(100%)
MOD= 0Hz/ 0%/.00T
POWER
SPECTRUM
0
10
20
30
40
50Hz
FREQUENCY

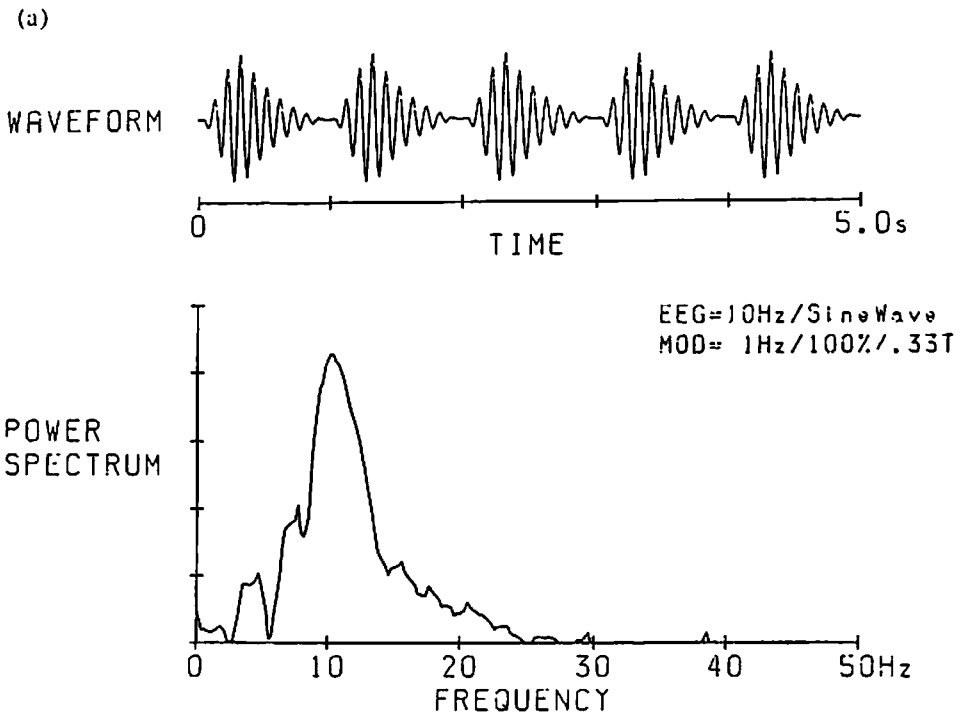

Fig.7. A set of waveforms and power spectra of the summated surface potentials as shown in Fig.6, modulated by a PSP wave of an infra-slow rhythm with different Tc values in the case of various modulation depths from 0 to 200% but the same among surface potentials. (a): a sinewave (100% modulation); (b): a positive surface potential (100%); (c): a biphasic surface potential (100%); (d): the same as (c) but the duty ratio of the modulator:0%; (e): the same as (d) but the ratio: 67%; (f): the same as (c) but in 50% modulation; (g): the same as (f) but 200% modulation.

(d)

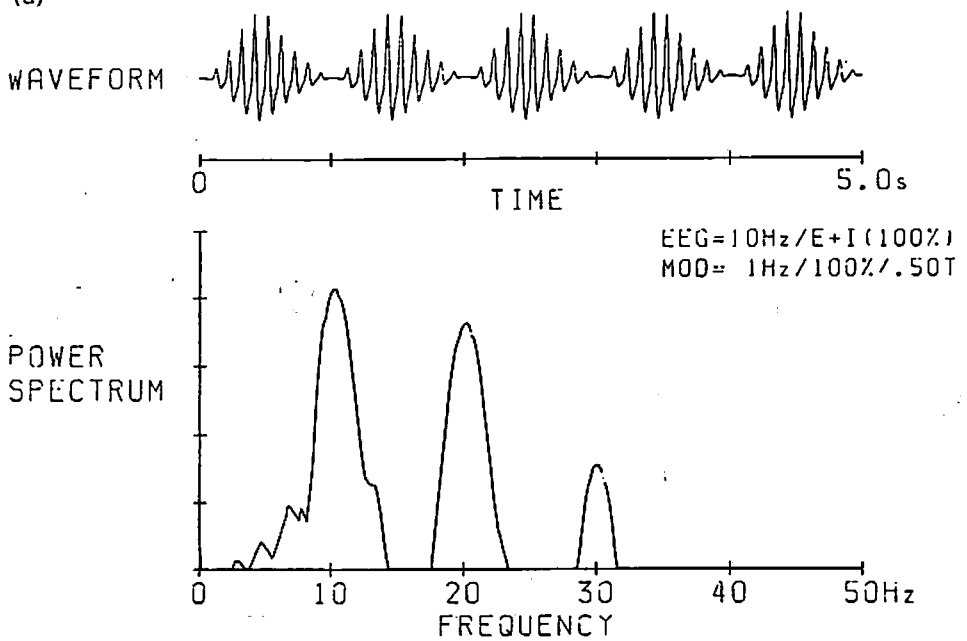
WAVEFORM
0
TIME
5.0s
EEG=10Hz/E+I(100%)
MOD= 1Hz/100%/.50T
POWER
SPECTRUM
0
10
20
30
40
50Hz
FREQUENCY

(e)

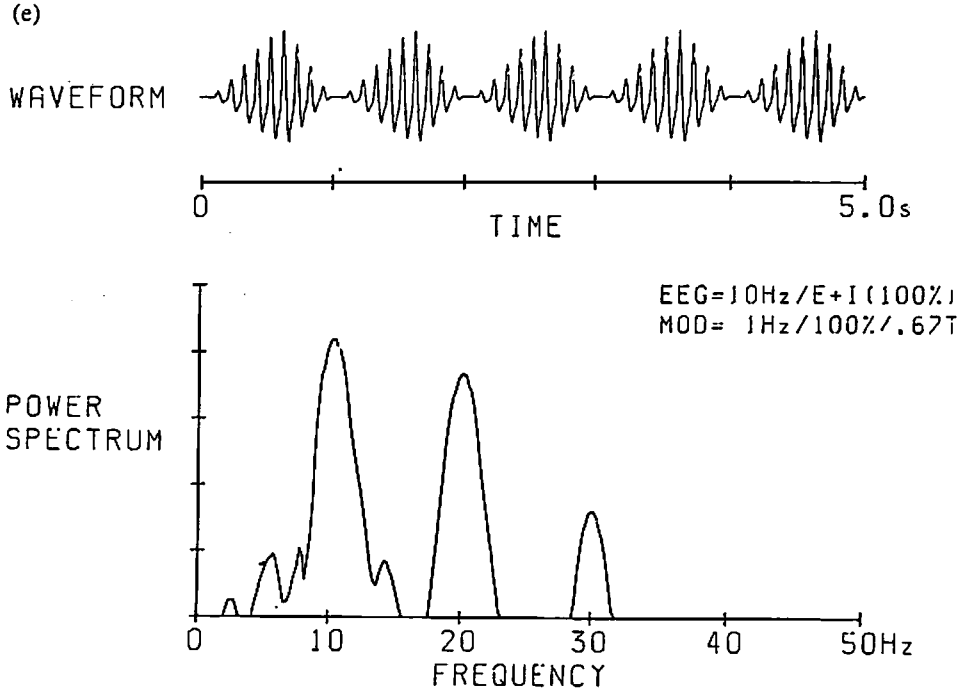
WAVEFORM
0
TIME
5.0s
EEG=10Hz/E+I(100%)
MOD= 1Hz/100%/.67T
POWER
SPECTRUM
0
10
20
30
40
50Hz
FREQUENCY

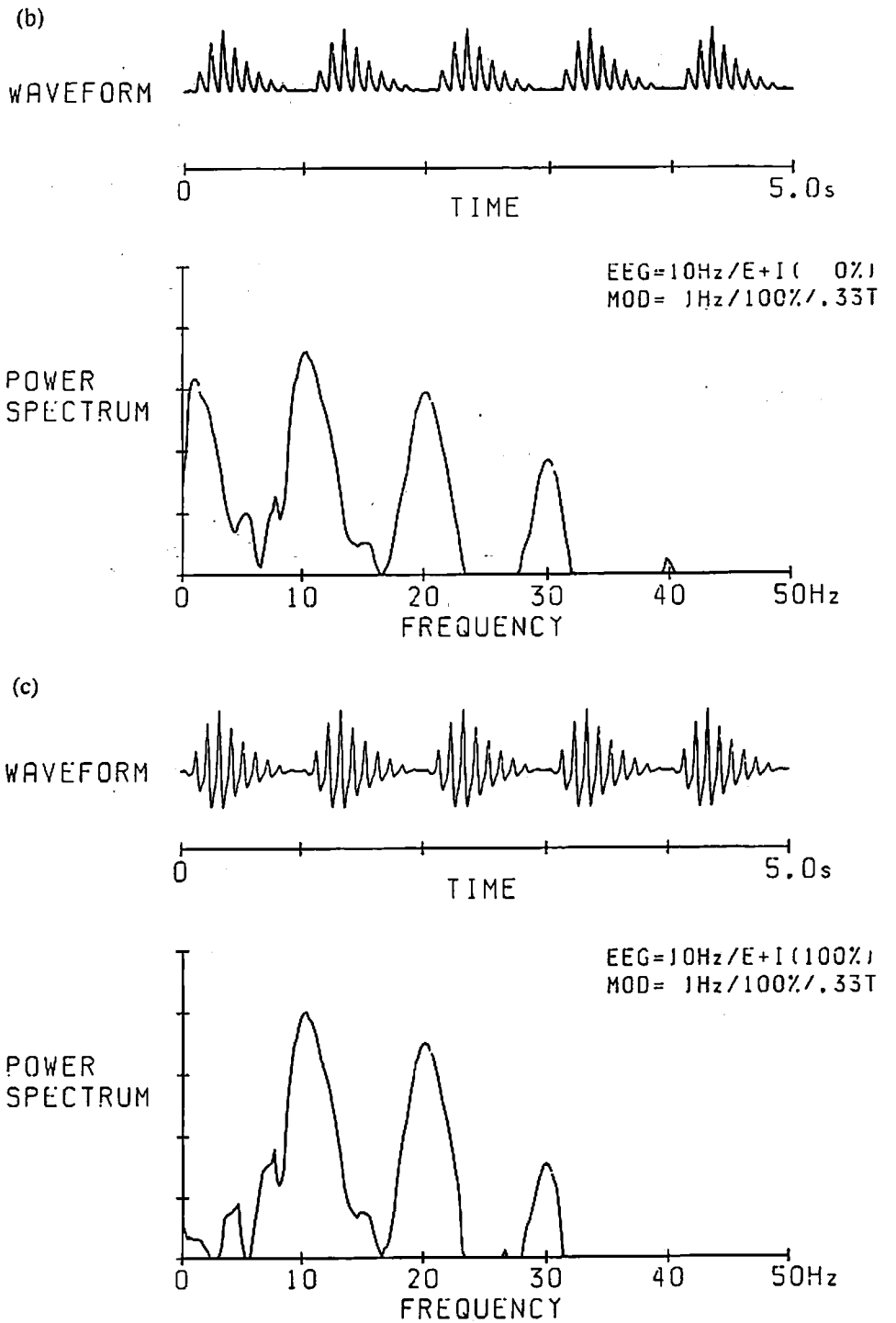
(b)
WAVEFORM
0
TIME
5.0s
EEG=10Hz/E+I(0%)
MOD= 1Hz/100%/.33T
POWER
SPECTRUM
0
10
20
30
40
50Hz
FREQUENCY
(c)
WAVEFORM
0
TIME
5.0s
EEG=10Hz/E+I(100%)
MOD= 1Hz/100%/.33T
POWER
SPECTRUM
0
10
20
30
40
50Hz
FREQUENCY

(f)

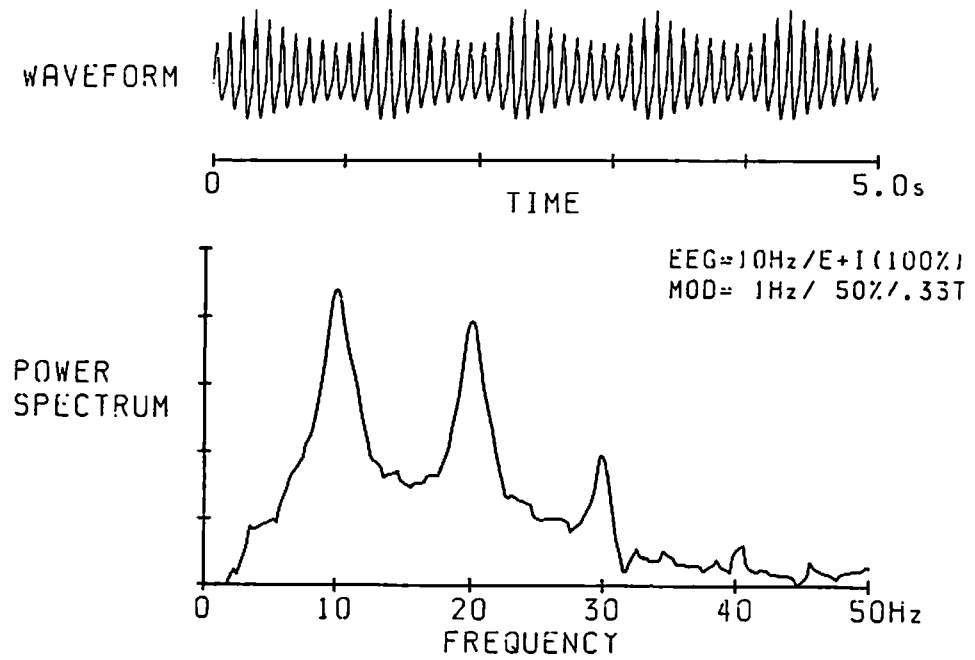
WAVEFORM
0
TIME
5.0s
EEG=10Hz/E+I(100%)
MOD= 1Hz/ 50%/.33T
POWER
SPECTRUM
0
10
20
30
40
50Hz
FREQUENCY

(g)

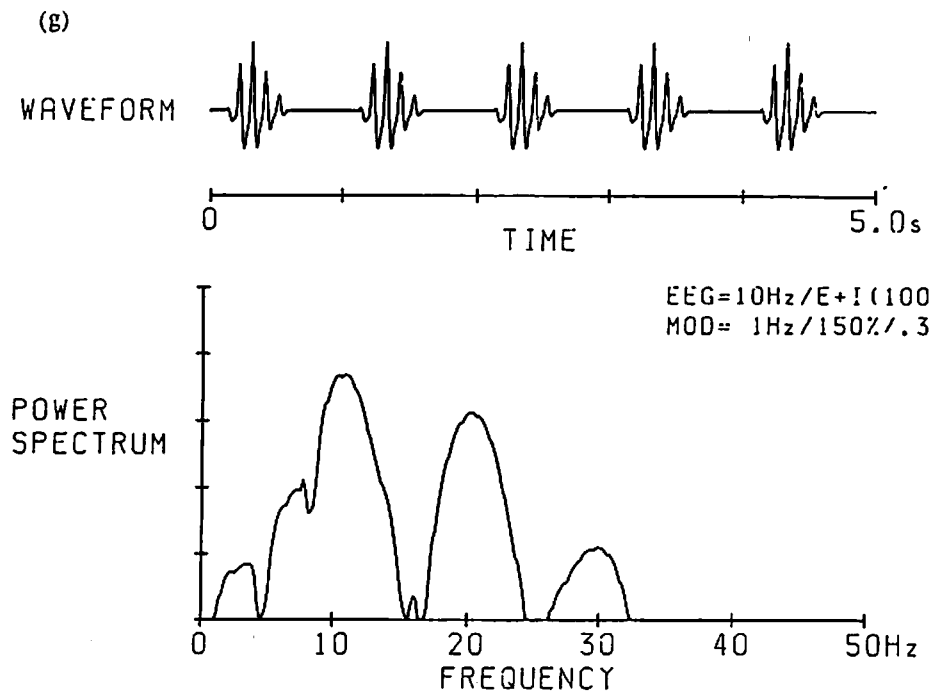
WAVEFORM
0
TIME
5.0s
EEG=10Hz/E+I(100%)
MOD= 1Hz/150%/.33T
POWER
SPECTRUM
0
10
20
30
40
50Hz
FREQUENCY

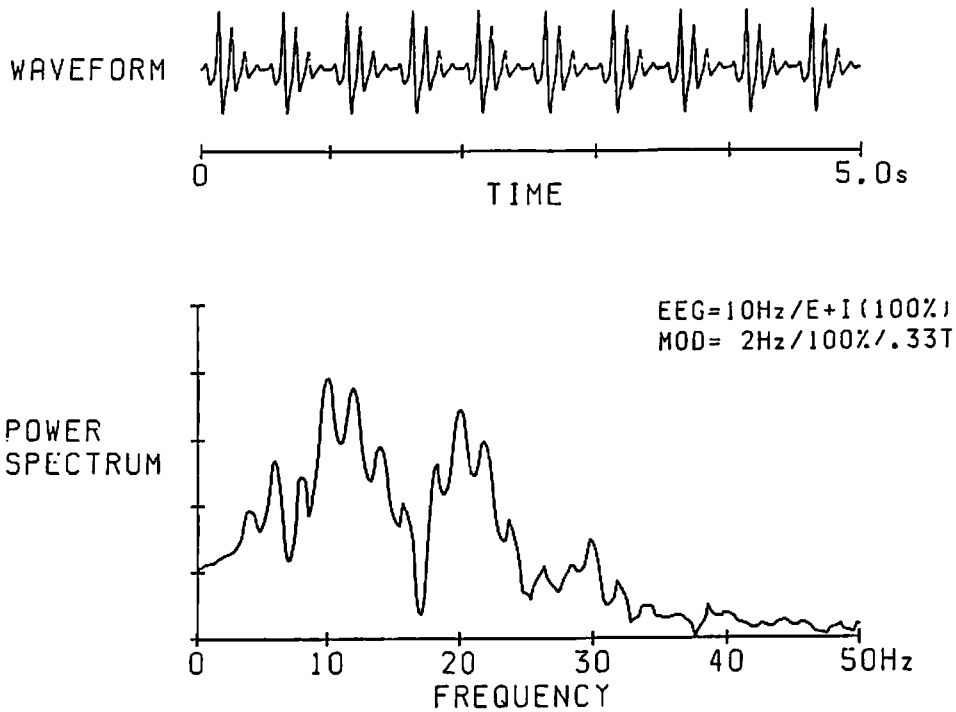

Fig.8. A set of waveforms and power spectra of the summated surface potentials with slow rhythm close to the modulator repetitive frequency.